Mechanics-Based Models to Predict the Alignment of Cells on a Cyclically Stretched Substrate

Mechanics-Based Models to Predict the Alignment of Cells on a Cyclically Stretched Substrate

Chiara Giverso, Giulio Lucci, and Luigi Preziosi

Abstract As pointed out by numerous experiments, the cell cytoskeleton appears to be responsive to external mechanical stimuli. In particular, experimental evidence demonstrates that a population of cells adhering to a substrate which is deformed periodically, for instance to mimic the heartbeat, responds to the strain by reorienting their stress fibres and focal adhesions. At the end of such a process, the cell achieves a specific orientation with respect to the strain direction, and such orientation depends on the characteristics of the external strain. The increasing interest in understanding mechanotransduction phenomena led to a growing attention to the cell realignment behaviour, both from the experimental and from the modelling point of view. Indeed, the contribution of mathematical models turns out to be very important to elucidate some relevant mechanisms and to suggest possible improvements in experimental assays. In this Chapter, we present an overview of mechanics-based mathematical models that have been proposed to describe cell reorientation and we highlight connections among the different research contributions within this field.

Chiara Giverso
Department of Mathematical Sciences "G.L. Lagrange", Politecnico di Torino, Corso Duca degli Abruzzi 24, I-10129 Turin, Italy
e-mail: chiara.giverso@polito.it

Giulio Lucci
Department of Mathematical Sciences "G.L. Lagrange", Politecnico di Torino, Corso Duca degli Abruzzi 24, I-10129 Turin, Italy
e-mail: giulio.lucci@polito.it

Luigi Preziosi
Department of Mathematical Sciences "G.L. Lagrange", Politecnico di Torino, Corso Duca degli Abruzzi 24, I-10129 Turin, Italy
e-mail: luigi.preziosi@polito.it

1 Phenomenological Observations

The response of cells to mechanical cues started to attract attention in the 1980s, following the study of cardiovascular pathophysiology. In particular, by observing the cellular arrangement in blood vessels, it was found that cells forming the walls of arteries were oriented along specific directions depending on their location. Endothelial cells in the innermost layer, in direct contact with blood flow, tended to be aligned in the axial direction of the vessel, while smooth muscle cells in deeper layers, e.g., in the intima and in the internal elastic lamina, exhibited an oblique or perpendicular orientation, forming helical-like structures, with cells sometimes disposed at an angle of 20°–40° with respect to the vascular axial direction [16]. The pulsatile behaviour of the heart and the arteries, whose cells are constantly exposed to periodic deformations, stimulated the first investigations *in vitro*, with the aim of gaining a deeper understanding of cell mechanosensitivity and orientation in the circulatory system.

Motivated by his own studies on the orientation of cells in aortic walls, Buck was the first to examine the response of cells to mechanical cues *in vitro* [4], by seeding a cell population on a rubber plastic substrate which was then cyclically stretched, to mimic the periodic vessel inflation during pulsatile flow. Similarly to cells *in vivo*, he found that nearly 81% of fibroblasts tended to reorient between 45° and 90° with respect to the stretching direction. This result attracted some interest since it firstly put in evidence such an alignment behaviour of stimulated cells *in vitro*, paving the way for successive investigations, as reviewed in detail in [14]. Remarkably, it was observed that the reorientation behaviour was almost cell-type independent, namely, epithelial cells, endothelial cells, fibroblasts, osteoblasts, melanocytes, mesenchymal stem cells, in addition to the already cited muscle-type cells, all responded in a similar way.

Specifically, in all experiments, it was observed that cells actively responded to the exerted stretch by reorienting and generating strongly linked actin bundles that are named stress fibres (SFs) oriented along specific directions, with a consequent morphological elongation of the cell in the same direction. The SFs are then linked to the external substrate by focal adhesion complexes, so that through them the cell is able to sense the mechanical deformation, to transfer the information inside the cell and to respond accordingly. In particular, it seems that, when submitted to an external stretch, the cell reorganizes its internal structure, in order to relieve the state of stress. A confirmation of the central role played by the cytoskeleton is given by the experiments performed by Wang et al. [40] who observed that the use of an inhibitor of cellular contractility disrupted stress fibres and blocked cell reorientation in response to cyclic stretching. For a similar reason, immune cells seem to be less responsive [26], since they do not possess a strong cytoskeleton and do not adhere firmly to the substrate. In fact, their role is to patrol the body for potential pathogens, and therefore to squeeze through endothelial linings with an amoeboid motion, with little involvement of adhesion molecules.

In addition to being a common response to several cell types, it seems that the phenomenon of cell realignment is nearly independent of the applied frequency and

amplitude of the periodic deformation, as well as of the stiffness of the substrate, provided that all these factors are large enough.

Starting from these phenomenological observations, the aim of this Chapter is to summarize the mechanics-based approaches which have been adopted so far to describe the cell realignment behaviour under stretch. Indeed, in recent years, several mathematical models have been proposed to target such a problem, with the purpose of better understanding mechanotransduction phenomena, which are still not fully elucidated.

In detail, after the introduction of some basic notation in Section 2, Sections 3 and 4 will examine the outcome of models based on the assumption that cells tend to minimize, respectively, either the strain or the stress acting on them. Along the same line, Section 5 will describe some models focusing on the minimization of a very general elastic energy, giving an explanation of why the equilibrium distribution of cells turns out to be so robust. Then, in Section 6 we will discuss a viscoelastic model, to give an explanation of the fact that, at low frequencies, the reorientation phenomenon is not observed.

2 Basic Notation

The two-dimensional set-ups that are typically used to test the behaviour of cells under stretch consist of a silicon or polydimetylsiloxane (PDMS) membrane, very often coated with collagen or fibronectin to favour cell attachment. Cells are then seeded on the substrate at a certain density: after that, the substrate is pulled along one or two perpendicular directions, either statically or periodically with different waveforms. In most of the experiments a cyclic stretch in only one direction is applied.

A simple pulling of two opposite sides would naturally lead to a narrowing in the central region, as shown in Fig. 1a, where the thin black lines refer to the undeformed square specimen, whereas the color map indicates the first principal strain in the deformed sample. In these cases, data are usually reported for those cells in the central region of the specimen (denoted by the dashed lines and shown magnified in the inset of Fig. 1a), where the stress and strain are almost homogeneous with principal directions along the direction of pulling and the perpendicular one.

So, assuming that the deformation applied to the substrate can be taken as purely extensional, the deformation gradient can be written as

$$\mathbb{F}(t) := \mathrm{diag}\{\lambda_x(t), \lambda_y(t), \lambda_z(t)\} = \mathrm{diag}\{1 + \delta_x(t), 1 + \delta_y(t), 1 + \delta_z(t)\}\,,$$

where x is the direction characterized by the maximum deformation, that will also be denoted in the following as the *main stretching direction*, and z is the direction perpendicular to the substrate plane. We also introduce the quantity $R(t)$ such that $\delta_y(t) = -R(t)\delta_x(t)$, that represents, for instance in static conditions, the percentage of contraction in the y-direction with respect to the extension in the x-direction. It is

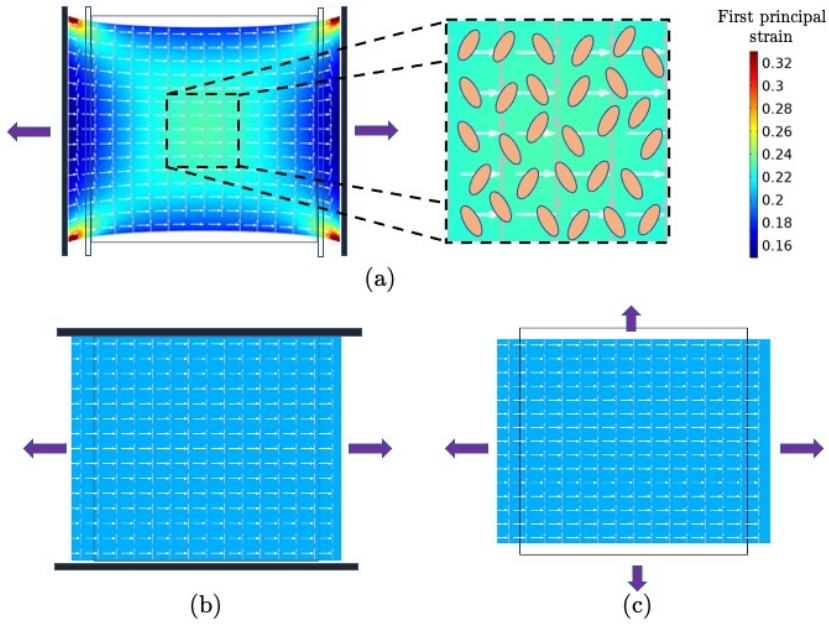

Fig. 1 Types of 2D deformations. In all panels, the thin black lines refer to the undeformed square specimen, whereas the colour plots refer to the first principal strain in the deformed sample. White and grey arrows represents the principal directions of the strain. The purple thick arrows represent the direction of the applied load/deformation. (a) Deformed substrate subject to a given deformation (10% strain) on two opposite sides while the others are stress-free. (b) Purely uniaxial stretching. (c) Simple elongation (when the top and bottom boundary of the specimen are stress-free) and biaxial deformation.

observed that during cyclic deformations $R(t)$ is nearly constant, so that an important parameter is the so-called *bi-axiality ratio*

$$r := -\frac{\max_t \delta_y(t)}{\max_t \delta_x(t)} .$$

In order to avoid the central narrowing of the specimen, some countermeasures are sometimes adopted, like thickening the borders parallel to the main stretching direction (as done, for instance, in [8]) or attaching that side to a more rigid structure or substratum. This procedure allows to have a larger region with the desired stress and strain fields, if not the entire specimen. If these borders are fixed as in Fig. 1b, then $\delta_y = r = 0$ and it is said that the specimen undergoes a *pure uniaxial stretching*. If they are allowed to move inwards while staying parallel to the main stretching direction, as in Fig. 1c, then $\delta_y < 0$ and $r > 0$, and it is said that the specimen undergoes a *simple elongation*. In any case, most experiments are performed with values of $r \in [0, 1]$. A negative value of r is obtained if the substrate is pulled in

both directions, as in [18, 21]. In particular, an equi-biaxial extension corresponds to $r = -1$. At the other extremum, a value larger than 1 corresponds to compression along y while pulling along x, which, to our knowledge, has not been done in experimental assays.

A cell that is oriented along a direction identified by a unit vector $\mathbf{N}$ undergoes a strain along that direction given by

$$\epsilon_N := \sqrt{(\mathbb{F}\mathbf{N}) \cdot (\mathbb{F}\mathbf{N})} - 1 = \sqrt{\mathbf{N} \cdot \mathbb{C}\mathbf{N}} - 1 := \sqrt{\mathrm{I}_4} - 1 \,, \tag{1}$$

where $\mathbb{C} := \mathbb{F}^{\mathrm{T}}\mathbb{F}$ is the right Cauchy-Green strain tensor, whereas $\mathrm{I}_4 := \mathbf{N} \cdot \mathbb{C}\mathbf{N}$ is known in elasticity as the fourth invariant that quantifies the squared stretch experienced in direction $\mathbf{N}$. If we work in two dimensions, so that we can denote $\mathbf{N} = (\cos\theta, \sin\theta, 0)$, then we have

$$\begin{aligned} \epsilon_N(t) &= \sqrt{[1+\delta_y(t)]^2 + [\delta_x(t) - \delta_y(t)][2 + \delta_x(t) + \delta_y(t)]\cos^2\theta} - 1 \\ &\approx \sqrt{[1 - r\delta_x(t)]^2 + [2 + (1-r)\delta_x(t)](1+r)\delta_x(t)\cos^2\theta} - 1 \,. \end{aligned} \tag{2}$$

In the small deformation regime, the infinitesimal strain tensor $\mathbb{E} := \mathrm{diag}\{\epsilon_{xx}, \epsilon_{yy}, \epsilon_{zz}\}$ is usually introduced and δ_i is replaced by ϵ_{ii}. Hence, $\mathbb{C} \approx \mathbb{I} + 2\mathbb{E}$, and $r \approx -\epsilon_{yy}/\epsilon_{xx}$. In this limit

$$\epsilon_N \approx \mathbf{N} \cdot \mathbb{E}\mathbf{N} = \epsilon_{xx}\cos^2\theta + \epsilon_{yy}\sin^2\theta = [(1+r)\cos^2\theta - r]\epsilon_{xx} := \hat{\mathrm{I}}_4\epsilon_{xx} \,, \tag{3}$$

as can be also obtained by linearizing Eq. (2). We notice that the term $\hat{\mathrm{I}}_4 = [(1+r)\cos^2\theta - r]$, which will appear in many models focusing on single stress fibres, is nothing else but the approximation of $\mathrm{I}_4 - 1$ in linear elasticity.

For the sake of simplicity, in the following we will denote ϵ_{xx} simply by ϵ and the maximum strain by $\epsilon_0 = \max_t \epsilon_{xx}(t)$.

3 Strain Avoidance

Historically, the first modelling approaches to describe cell reorientation under stretch were based on a strain minimization principle, which led to naming the phenomenon as *strain avoidance*. According to this simple hypothesis, the cell preferentially reorients in the direction where the minimum strain is sensed. A direct application of this principle to Eq. (2), or (3), readily leads to the fact that the only stable equilibrium should satisfy

$$\cos^2\theta_{eq} = \frac{r}{1+r} \,.$$

With respect to this trivial approach, Wang et al. [37] assumed that there was a maximum strain $\bar{\epsilon}_N$ that can be sustained by cells. As a consequence, the cell avoids

any direction along which the perceived strain is greater than the maximum threshold. So, by considering the maximum strain δ_0 and inverting Eq. (2) they obtained the condition

$$\cos^2\theta \leq \frac{2\bar{\epsilon}_N + \bar{\epsilon}_N^2 + 2r\delta_0 - r^2\delta_0^2}{[2+(1-r)\delta_0](1+r)\delta_0}, \tag{4}$$

which determines a critical angle

$$\theta_{cr} = \cos^{-1}\sqrt{\frac{2\bar{\epsilon}_N + \bar{\epsilon}_N^2 + 2r\delta_0 - r^2\delta_0^2}{[2+(1-r)\delta_x](1+r)\delta_0}}.$$

Actually, in [37] the $\bar{\epsilon}_N^2$ term is not present, probably due to an approximation or to the fact that they use the Green-Lagrange tensor $\mathbb{G} = \frac{1}{2}(\mathbb{C} - \mathbb{I})$ as deformation measure. This approach was later applied in [27], where Eq. (2) is written (but with a misprinted sign and two ξ's that should be δ's).

In [38], the model by Wang was a bit more elaborated and accounted for actin filament dynamics. More in detail, he evaluated the change in the strain energy of a fibre due to the action of the axial strain ϵ_f transmitted to it. It was also assumed that only a fraction of the substrate strain was effectively transferred to the filaments, that is, $\epsilon_f = \alpha_t\epsilon_N$ in tension and $\epsilon_f = \alpha_c\epsilon_N$ in compression, with $\alpha_t < \alpha_c$ and ϵ_N as in Eq. (2). The model is then proposed under the following assumptions:

(i) in the absence of deformation, each filament of actin owns a basal strain energy given by $E_b = k\delta^2/2$, where δ is the pre-strain of the SF due to its inherent tension; then, the total energy of the fibre is $E_f = k(\delta + L\epsilon_f)^2/2$, where L is the initial length of the filament;
(ii) only the normal substrate strain ϵ_N is transmitted to individual actin filaments;
(iii) the actin filaments cannot bear compression;
(iv) the actin filaments undergo disassembly if their strain energy E_f is changed to zero or to a value greater than twice their basal strain energy E_b.

The limits in assumption (iv) are crucial because they allow to identify through Eq. (3) an interval of admissible orientations

$$\theta \in \left[\cos^{-1}\sqrt{\frac{r}{1+r} + \frac{(\sqrt{2}-1)\delta}{(1+r)\alpha_t L\epsilon}},\ \cos^{-1}\sqrt{\frac{r}{1+r} - \frac{\delta}{(1+r)\alpha_c L\epsilon}}\right]. \tag{5}$$

Then, to simplify the resulting formulas, it is conveniently assumed that the relation $\alpha_t = (\sqrt{2}-1)\alpha_c$ between coefficients holds.
In the limit $\frac{\delta}{\alpha_t L\epsilon}, \frac{\delta}{\alpha_c L\epsilon} \to 0$ the interval in Eq. (5) collapses to the point

$$\theta_{eq} = \cos^{-1}\sqrt{\frac{r}{1+r}} = \tan^{-1}\sqrt{\frac{1}{r}}, \tag{6}$$

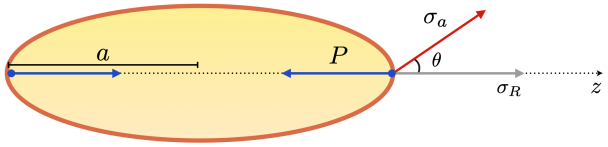

Fig. 2 Sketch of the cell dipole description used in some models of realignment. The variables of the model are the contractile dipole force $P < 0$ and the angle θ at which the external stress σ_a is applied.

while its width increases when the above values increase and, in particular, if ϵ decreases. Conversely, according to this model, increasing ϵ (without going into conflict with the small strain hypothesis) leads to a narrowing of the range of angles for which filament disassembly does not occur. This intriguingly well correlates with the fact that higher strain amplitudes lead to narrower ranges of measured orientation angles, and therefore to more peaked distribution probabilities of the orientation. A similar approach was also used in [3] and [13].

A slightly different approach, though still within the strain avoidance class, was used by De and coworkers [10, 11]. In particular, using a coarse-grained model, they consider the cell as a force dipole (sketched in Fig. 2) to mimic the contraction of stress fibres along a given direction. Then, it is assumed that cell reorganisation happens with the aim of reaching an optimal level of strain ϵ_{target}. As a consequence, a reaction strain in the surrounding matrix is identified:

$$\epsilon_R = -\frac{(1+r)P}{\pi a^3 E}\,,$$

where P is the (negative) cell contractile dipole magnitude, E is the Young modulus of the matrix and a is the cell size. Instead, the component of the applied strain along the cell axis is

$$\epsilon_a = \frac{\sigma_a}{E}\hat{\mathrm{I}}_4\,, \tag{7}$$

with σ_a the external uniaxial applied stress. Starting from these considerations, a free energy is built:

$$\mathcal{U}_\varepsilon = \mathcal{U}_{\text{cell},\epsilon} + \mathcal{U}_{\text{self}} + \mathcal{U}_{\text{int}}\,,$$

where

$$\begin{aligned}
\mathcal{U}_{\text{cell},\epsilon} &= \frac{1}{2}\chi\left[\frac{\sigma_a}{E}\hat{\mathrm{I}}_4 - \frac{P(1+r)}{\pi a^3 E} - \epsilon_{\text{target}}\right]^2\,,\\
\mathcal{U}_{\text{self}} &= (1+r)\frac{10r^2-14r+9}{30(1-r)^2}\frac{P^2}{2\pi a^3 E}\,,\\
\mathcal{U}_{\text{int}} &= P\frac{\sigma_a}{E}\hat{\mathrm{I}}_4\,.
\end{aligned} \tag{8}$$

In detail, the contribution $\mathcal{U}_{\text{cell},\epsilon}$ is the free energy related to the contractile activity of the cell, which is minimized when $\epsilon_a + \epsilon_R = \epsilon_{\text{target}}$, i.e. when the cell feels the optimal strain. On the other hand, $\mathcal{U}_{\text{self}}$ gives rise to a force that tends to reduce the magnitude of the dipole [10], whereas $\mathcal{U}_{\text{int}}$ represents the interaction between the dipole and the external strain. The variables of the model are therefore P and θ, with a dynamics assumed to be given by [11]:

$$\frac{dP}{dt} = -\frac{1}{\tau_P}\frac{\partial \mathcal{U}_\epsilon}{\partial P}\,, \quad \frac{d\theta}{dt} = -\frac{1}{\tau_\theta}\frac{\partial \mathcal{U}_\epsilon}{\partial \theta}\,. \tag{9}$$

Actually, in a subsequent work [10], the equation for θ is modified by multiplying for a factor $1/P^2$, even though the results are only altered slightly. When a cyclic deformation with a high frequency is applied, in the form $\sigma_a(t) = \sigma_a(1 - \cos\omega t)$, the energy may be averaged over a period, since the cell is not able to follow the stress instantaneously. The resulting averaged energy has an additional contribution, namely,

$$\langle \mathcal{U}_\epsilon \rangle = \mathcal{U}_{\text{cell},\epsilon} + \mathcal{U}_{\text{self}} + \mathcal{U}_{\text{int}} + \mathcal{U}_{\text{av},\epsilon}\,, \tag{10}$$

in which the first three terms have the same form as Eq. (8) and

$$\mathcal{U}_{\text{av},\epsilon} = \frac{1}{4}\chi\left(\frac{\sigma_a}{E}\hat{\mathrm{I}}_4\right)^2\,. \tag{11}$$

The stationary solutions can be derived by imposing that the derivatives of such an energy with respect to both P and θ are null. These steady state solutions are found to be $\theta_{eq} = 0$, $\theta_{eq} = \pi/2$ and an oblique one, which is defined in terms of its squared cosine by the implicit relation:

$$\cos^2\theta_{eq} = 1 + \frac{P_{eq}(\theta_{eq})}{\pi a^3 \sigma_a} - \left(1 + \frac{E P_{eq}(\theta_{eq})}{\chi\sigma_a} - \frac{E\epsilon_{\text{target}}}{\sigma_a}\right)\frac{1}{1+r}\,, \tag{12}$$

in a suitable range of parameters. In particular, if the interaction forces with the extracellular matrix are negligible, one can assume that $P \approx 0$ and, if $\epsilon_{\text{target}} = 0$ is taken, Eq. (6) is recovered from Eq. (12).

As we will discuss in Section 4, the same authors also explored the possibility that cell remodelling aims at reaching a target stress rather than a target strain.

As a final remark, we mention that the dipole approach has been generalized to the case of several cells in [43], while in [9], still in the same framework, more attention is paid to the dynamics of focal adhesions. A generalization of the dipole approach is also proposed in [29] to investigate the cell response to point loads.

4 Stress Avoidance

Within the same framework as the one discussed in Section 3, in [11, 12, 34] the alternative hypothesis of *stress avoidance* is examined. Specifically, it is assumed

that the cell attempts to reach a target stress rather than a target strain by means of its contractile activity. In this case, the reaction stress in the matrix writes as

$$\sigma_R = -\frac{2-r}{1-r}\frac{P}{2\pi a^3}\,,$$

with the same notation as above. The force component due to the applied stress on the surrounding matrix along the direction of the cell axis is given by $\sigma_a \cos^2\theta$. The free energy of the system, which includes the active contribution from the cell cytoskeleton and the forces acting on the cellular dipole due to the elasticity of the matrix, becomes

$$\mathcal{U}_\sigma = \mathcal{U}_{\text{cell},\sigma} + \mathcal{U}_{\text{self}} + \mathcal{U}_{\text{int}}\,,$$

where

$$\mathcal{U}_{\text{cell},\sigma} = \frac{1}{2}\chi\left(\sigma_a\cos^2\theta - \frac{2-r}{1-r}\frac{P}{2\pi a^3} - \sigma_{\text{target}}\right)^2$$

is the active energy of the cell, whereas the contributions due to the interactions of the dipole with the surrounding matrix and the external stress are the same as in Eq. (8). Instead, σ_{target} identifies the target stress of the cell, so that $\mathcal{U}_{\text{cell},\sigma}$ is minimized if the sum of the reactive stress σ_R and the applied stress σ_a is equal to the target. If an averaging over a cycle is performed, the energy becomes

$$\langle\mathcal{U}_\sigma\rangle = \mathcal{U}_{\text{cell},\sigma} + \mathcal{U}_{\text{self}} + \mathcal{U}_{\text{int}} + \mathcal{U}_{\text{av},\sigma} \qquad \text{with} \qquad \mathcal{U}_{\text{av},\sigma} = \frac{1}{4}\chi\sigma_a^2\cos^4\theta\,.$$

The equilibrium orientations of the system, i.e. the solutions of Eq. (9), are then identified with $\theta_{eq} = 0$, $\theta_{eq} = \pi/2$ and an oblique orientation defined in general by the implicit relation

$$\cos^2\theta_{eq} = \frac{2}{3}\left[\frac{2-r}{1-r}\frac{P_{eq}(\theta_{eq})}{2\pi a^3\sigma_a} + \frac{\sigma_{\text{target}}}{\sigma_a} - \frac{P_{eq}(\theta_{eq})}{\chi E\sigma_a}(1+r)\right]\,. \tag{13}$$

It should be noticed that there are strong constraints, especially on r, for the existence of such an oblique equilibrium. For instance, it might not exist for values of r suitably close to 1, which correspond to a 2D incompressible situation. It is also worth to point out that, if solely the energy of the cell is considered, i.e. $\mathcal{U}_{\text{self}}$ and $\mathcal{U}_{\text{int}}$ are neglected, the only equilibrium orientations are $\theta_{eq} = 0$ and $\theta_{eq} = \pi/2$. The latter is the stable one and corresponds to the direction of minimal stress, if a uniaxial applied stress is considered. The authors then study the response of such a dipole model to external stresses, both in static and cyclic conditions [10, 11].

5 Elastic Energy Approach

Both the approaches based on strain avoidance and stress avoidance have been questioned by experimental data obtained by Livne et al. [22], who performed a wide series of experiments carefully controlling the biaxiality ratio. It was shown in particular that neither the strain nor the stress avoidance-based laws for the preferential angle of the cell were able to reproduce the experimental data found in [22]. Instead, a change of perspective was proposed in their work, suggesting that the cell attempts to minimize the stored elastic energy, rather than the strain. This choice allowed to obtain a better fitting of the orientations found experimentally.

Before discussing further this approach, it is useful to observe that, since a cell does not have a real polarization given by a head and a tail during the reorientation process, configurations with cells aligned along θ and $\theta+\pi$ are geometrically indistinguishable and therefore also equivalent from the energetic point of view, i.e. $\mathcal{U}(\theta+\pi)=\mathcal{U}(\theta)$, where $\mathcal{U}$ is the elastic energy. In addition, also the orientation of the axis is equivalent and, as a consequence, $\mathcal{U}(\pi-\theta)=\mathcal{U}(\theta)$. So, in conclusion, $\mathcal{U}(\theta)$ is an even π-periodic function, so that

$$\mathcal{U}(\theta)=\mathcal{U}(2\pi-\theta)=\mathcal{U}(\pi-\theta)=\mathcal{U}(\pi+\theta),\quad \forall\theta. \tag{14}$$

Let us then recall that, generally speaking, denoting by $\mathbf{N}_\perp=(-\sin\theta,\cos\theta,0)$ the orientation perpendicular to $\mathbf{N}=(\cos\theta,\sin\theta,0)$ on the substratum, a general elastic energy density for an orthotropic material can depend on the invariants [28, 35]

$$\begin{aligned}
&\mathrm{I}_4:=\mathbf{N}\cdot\mathbb{C}\mathbf{N}=(\lambda_x^2-\lambda_y^2)\cos^2\theta+\lambda_y^2\,, && \mathrm{I}_5:=\mathbf{N}\cdot\mathbb{C}^2\mathbf{N}=(\lambda_x^4-\lambda_y^4)\cos^2\theta+\lambda_y^4\,,\\
&\mathrm{I}_6:=\mathbf{N}_\perp\cdot\mathbb{C}\mathbf{N}_\perp=\lambda_x^2-(\lambda_x^2-\lambda_y^2)\cos^2\theta\,, && \mathrm{I}_7:=\mathbf{N}_\perp\cdot\mathbb{C}^2\mathbf{N}_\perp=\lambda_x^4-(\lambda_x^4-\lambda_y^4)\cos^2\theta\,,\\
&\mathrm{I}_8:=\mathbf{N}_\perp\cdot\mathbb{C}\mathbf{N}=-(\lambda_x^2-\lambda_y^2)\sin\theta\cos\theta\,,
\end{aligned} \tag{15}$$

in addition to the usual invariants characterizing an isotropic material

$$\mathrm{I}_1:=\operatorname{tr}\mathbb{C},\qquad \mathrm{I}_2:=\frac{1}{2}\left[(\operatorname{tr}\mathbb{C})^2-\operatorname{tr}\mathbb{C}^2\right],\qquad \text{and}\qquad \mathrm{I}_3:=\det\mathbb{C}\,,$$

that do not depend on the angle θ. We notice that all the invariants in Eq. (15) except I_8 satisfy a priori the symmetry conditions in Eq. (14). Therefore, as an additional requirement on $\mathcal{U}$, we assume it to be an even function of I_8, e.g. a function of $\mathrm{I}_8^2=(\lambda_x^2-\lambda_y^2)^2(1-\cos^2\theta)\cos^2\theta$. Under this assumption, the energy becomes a function of the angle only through its squared cosine, i.e. $\mathcal{U}=U(\cos^2\theta)$, and the stationary points are trivially identified by

$$U'(\cos^2\theta)\sin\theta\cos\theta=0\,. \tag{16}$$

Therefore, one always has the trivial equilibrium orientations $\theta_{eq} = 0$ and $\theta_{eq} = \pi/2$, whereas further equilibria might exist, depending on the specific energy considered, for the values of $\theta_{eq} = \hat{\theta}$ such that $U'\left(\cos^2\hat{\theta}\right) = 0$.

Stability of these configurations is achieved if they correspond to minima of the elastic energy, and therefore it depends on the positivity of $U''(\cos^2\theta)\sin^2\theta\cos^2\theta - U'(\cos^2\theta)(\cos^2\theta - \sin^2\theta)$ computed at equilibrium. So, one has the following general stability conditions:

$$\begin{aligned} \theta = 0: &\quad \text{stable} \quad \Longleftrightarrow U'(1) < 0\,, \\ \theta = \frac{\pi}{2}: &\quad \text{stable} \quad \Longleftrightarrow U'(0) > 0\,, \\ \theta = \hat{\theta}: &\quad \text{stable} \quad \Longleftrightarrow U''\left(\cos 2\hat{\theta}\right) > 0\,, \end{aligned} \tag{17}$$

whenever the last position exists. In the next Subsections, we will specialize the elastic energy approach in the framework of both linear (see Section 5.1) and nonlinear elasticity (see Section 5.2). Finally, we will look at the evolution in time of the angle θ in Section 5.3.

5.1 Linear Elasticity

If linear elasticity is used, as done by Livne et al. [22], the most general elastic energy satisfying the symmetry properties in Eq. (14) can be written as (see [23])

$$\begin{aligned} U(\mathbb{E}, \mathbf{N}, \mathbf{N}_\perp) = 2K'_\parallel(\mathrm{tr}\,\mathbb{E})\mathbf{N}\cdot\mathbb{E}\mathbf{N} + 2K'_\perp(\mathrm{tr}\,\mathbb{E})\mathbf{N}_\perp\cdot\mathbb{E}\mathbf{N}_\perp + \frac{1}{2}K_\parallel(\mathbf{N}\cdot\mathbb{E}\mathbf{N})^2 \\ + \frac{1}{2}K_\perp(\mathbf{N}_\perp\cdot\mathbb{E}\mathbf{N}_\perp)^2 + \frac{1}{2}K_\phi(\mathbf{N}_\perp\cdot\mathbb{E}\mathbf{N})^2 + K_{\parallel\perp}(\mathbf{N}\cdot\mathbb{E}\mathbf{N})(\mathbf{N}_\perp\cdot\mathbb{E}\mathbf{N}_\perp)\,, \end{aligned} \tag{18}$$

where $K_\parallel$ is a coefficient related to the cell mechanical response to stretching in the direction of its main stress fibre orientation, $K_\perp$ to the one in the orthogonal direction, and K_ϕ to the one related to shear. The other coefficients are due to mixing effects.

In terms of θ, Eq. (18) then writes

$$\begin{aligned} U(\epsilon,\theta) = 2\epsilon^2(1-r)\Big[(K'_\parallel - K'_\perp)\xi(\theta) + (K'_\perp - rK'_\parallel)\Big] + \frac{1}{2}\epsilon^2\Big\{K_\parallel[\xi(\theta)-r]^2 \\ + K_\perp[1-\xi(\theta)]^2 + K_\phi\,\xi(\theta)[r+1-\xi(\theta)] + 2K_{\parallel\perp}[\xi(\theta)-r][1-\xi(\theta)]\Big\}\,, \end{aligned} \tag{19}$$

where $\xi(\theta) := (r+1)\cos^2\theta$.

We remark that the use of discrete models focusing on the behaviour of stress fibres aligned along a direction θ, as done for instance in [11, 12, 34], is equivalent to considering an energy that only depends on I_4 (see Eqs. (1) and (3)).

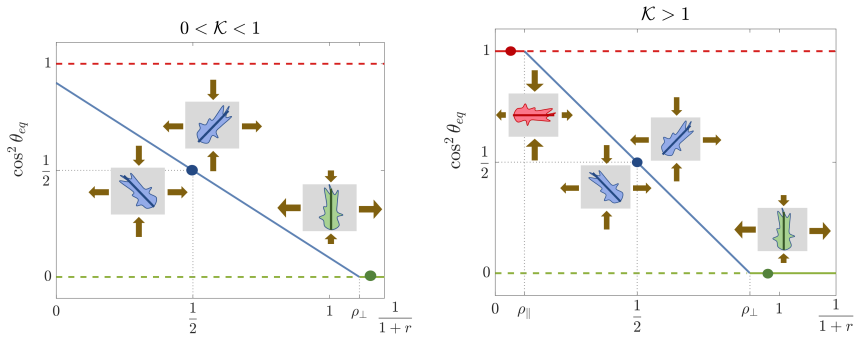

(a) (b)

Fig. 3 Bifurcation diagrams for $\mathcal{K} > 0$, with $0 < \mathcal{K} < 1$ in (a) and $\mathcal{K} > 1$ in (b). Solid lines indicate stable orientations, whereas dashed lines identify unstable positions. The insets and dots in (a) and (b) show representative cellular orientations: perpendicular (green), oblique (blue) and parallel (red). The arrows indicate the directions of stretching or compression.

Recalling the general observations for the stationary points of the energy given by Eq. (16), for an elastic energy in the form of Eq. (19), the equilibrium orientations are found to be $\theta_{eq} = 0, \frac{\pi}{2}$ and the oblique ones satisfying

$$\cos^2\theta_{eq} = \frac{1}{2} + \mathcal{K}\left(\frac{1}{2} - \frac{1}{1+r}\right), \tag{20}$$

where

$$\mathcal{K} := \frac{K_\parallel - K_\perp + 4(K'_\parallel - K'_\perp)}{K_\parallel + K_\perp - K_\phi - 2K_{\parallel\perp}}. \tag{21}$$

This is a generalisation of the linear relation firstly found by Livne et al. [22] starting from a simple linear elastic energy:

$$\cos^2\theta_{eq} = b + \frac{1-2b}{1+r}, \tag{22}$$

where b is a material parameter. Therefore, we can argue that the linear relation defined in Eq. (22) holds true even if a very general linear elastic orthotropic model is considered. The only difference is that more coefficients contribute to the slope of the line defined by Eq. (20).

Moreover, the stability of the equilibrium orientations of the cell can be reported on bifurcation diagrams as the ones shown in Fig. 3. In particular, for $\mathcal{K} > 0$ we find two supercritical bifurcation points at

$$\frac{1}{1+r} = \rho_\parallel := \frac{1}{2}\left(1 - \frac{1}{\mathcal{K}}\right) \quad \text{and} \quad \frac{1}{1+r} = \rho_\perp := \frac{1}{2}\left(1 + \frac{1}{\mathcal{K}}\right).$$

In particular, as $(1+r)^{-1}$ crosses $\rho_{\parallel}$, the oblique orientation (blue line) appears and becomes the only stable one. Instead, for $(1+r)^{-1} > \rho_{\perp}$, the oblique orientation does not exist and the stable alignment is perpendicular to the main stretch direction (green line). We remark that $\rho_{\parallel}$ is negative if $0 < \mathcal{K} < 1$.

Conversely, from Eq. (20), for an imposed $r \neq 1$ and for a measured $\theta_{eq} \neq 0$, $\theta_{eq} \neq \frac{\pi}{2}$, one can estimate the material parameter $\mathcal{K}$ by using

$$\mathcal{K} = -\frac{1+r}{1-r}\cos 2\theta_{eq}\,. \tag{23}$$

Data obtained using fibroblasts reported in [22] suggest that $\mathcal{K} \approx 1.26 \pm 0.08$. One could then ask whether such a value is universal, that is, independent of the cell type and the substratum of the specific experiment in sub-confluent conditions (since the confluent case might lead to differences [15]). In this respect, the bifurcation diagram in Fig. 3 puts in evidence that, if $\mathcal{K} > 1$, the only stable solution for $\frac{1}{1+r} > \rho_{\perp}$, and therefore $r > \frac{1}{\rho_{\perp}} - 1$, is $\theta_{eq} = \frac{\pi}{2}$. This includes the case in which $\epsilon_{yy} = r = 0$. Now, some pure uniaxial experiments (for which $r = 0$) seem instead to put in evidence that $\theta_{eq} \neq \frac{\pi}{2}$, suggesting that it may also be $\mathcal{K} < 1$. On assuming that $\theta_{eq}(r=0) = \theta_0 \neq \frac{\pi}{2}$, Eq. (23) gives

$$\mathcal{K} = -\cos 2\theta_0\,. \tag{24}$$

This suggests that the best way to evaluate the parameter $\mathcal{K}$ is to perform careful pure uniaxial experiments and, if $\theta_{eq} \neq 0$, determine it by using Eq. (24). For instance, Wang et al. [41] present results for $r = 0$ stating that the preferential orientation is perpendicular to the main strain direction, but from their Fig. 3A and Fig. 3B cells seem to have an alignment between 70° and 80°, which corresponds to a value of $\mathcal{K} \in [0.766, 0.936]$. Similarly, the interval of $\theta_{eq} \in [80°, 85°]$ found in the experiments in [39, 41] for $r = 0$ would lead to an evaluation of $\mathcal{K} \in [0.936, 0.985]$. On the other hand, when cells are oriented perpendicularly for $r = 0$, as for instance in [25], we can only argue that $\mathcal{K} > 1$.

Furthermore, in another work, Wang et al. [40] observed that, in the presence of the drug N-acetylcysteine, cells reoriented to an angle close to 70°, while for the control case the preferential angle was close to 85°. This result might indicate that N-acetylcysteine interferes with the mechanical machinery of the cell: in model terms, such an effect can be translated into a change in the coefficients of the elastic energy. Specifically, accounting for the fact that $r = 0$, the change in angle corresponds to a decrease from $\mathcal{K} \approx 0.98$ to $\mathcal{K} \approx 0.77$, and therefore to a decrease (in absolute value) in the steepness of the straight line in Fig. 3.

Another observation is that, if we invert Eq. (20) to write

$$r = \frac{\mathcal{K} + \cos 2\theta_{eq}}{\mathcal{K} - \cos 2\theta_{eq}}\,,$$

and we take for instance the slope indicated by the experiments in [22], then an equilibrium $\theta_{eq} \in [80°, 100°]$ is achieved for $r < 0.146$. So, a wide range of values

for r would lead to an almost perpendicular orientation. This might explain why, in many papers, one has a description that only refers to a perpendicular arrangement, without specifying the precise angle of orientation.

Finally, we conclude this Section with a remark about the minimum number of parameters necessary to model the reorientation behaviour. In particular, we can observe that having only $K_\parallel \neq 0$ in Eq. (21) would give $\mathcal{K} = 1$. Then, adding only a non-vanishing $K_\perp$ would decrease $\mathcal{K}$ to $\mathcal{K} < 1$. In order to have $\mathcal{K} > 1$, as observed for instance in [22], it is sufficient to include a non-vanishing K_ϕ, i.e., a response to shear, or alternatively a positive coupling term $K'_\parallel$ between the invariants I_1 and I_4. In any case, taking as an example the value suggested by the experiments in [22], one can evaluate

$$\frac{K_\phi}{K_\parallel} \approx 0.21\,,$$

in the first case, or

$$\frac{K'_\parallel}{K_\parallel} \approx 0.065\,,$$

in the second case. In particular, we can argue that a small contribution of the mixed term $K'_\parallel$ is enough to recover the experimental values.

5.2 Nonlinear Elasticity

The fact that in some experiments the applied strain can be higher than 30% [13, 22] suggests to drop the linear elasticity assumption and to see why also in this nonlinear regime the equilibrium orientation appears to be the same. Actually, a result very similar to Eq. (20) is reached in [24] starting from the following quite general nonlinear constitutive orthotropic model

$$\hat{U} = \frac{1}{2}\mathbf{I}\cdot\mathbb{K}\mathbf{I} + \mathcal{V}\,, \tag{25}$$

where $\mathbf{I} := (\mathrm{I}_4 - 1, \mathrm{I}_5 - 1, \mathrm{I}_6 - 1, \mathrm{I}_7 - 1, \mathrm{I}_8)^{\mathrm{T}}$ and $\mathbb{K}$ is the symmetric matrix of coefficients (that might possibly depend on the isotropic invariants), while $\mathcal{V}$ is the purely isotropic contribution that depends on $(\mathrm{I}_1, \mathrm{I}_2, \mathrm{I}_3)$. It is also observed that the same results are achieved with a Fung-type energy of the form

$$U_F = C\left(\exp\hat{U} - 1\right)\,, \tag{26}$$

that is often used in biomechanical applications.

In spite of the nonlinear framework and of the generality of the elastic energy, in [24] equilibria are explicitly determined together with their stability and a bifurcation analysis is fully discussed. In summary, it is proved that:

- The symmetry requirements in Eq. (14) imply that the coefficients coupling I_8 with the other invariants must vanish;

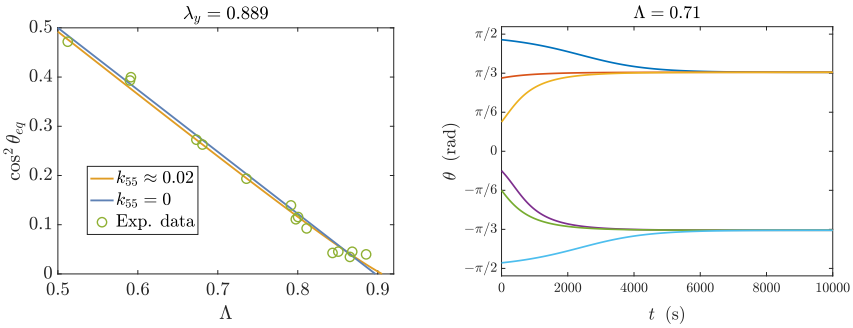

Fig. 4 (a): Comparison of experimental data from [13] and [22] for $\lambda_y = 0.889$ taking $k_{55} = 0$ and the best fitting value $k_{55} \approx 0.02$. (b): Evolution of the angle in time for $\Lambda = 0.71$ and $k_{55} = 0.02$, for different initial conditions.

- If the energy is independent of the invariants involving $\mathbb{C}^2$, namely I_5 and I_7, equilibria are given by a formula akin to Eq. (20), with $\dfrac{1}{1+r}$ replaced by its nonlinear generalization $\Lambda := \dfrac{\lambda_x^2 - 1}{\lambda_x^2 - \lambda_y^2}$;
- The inclusion of the dependence on I_5 induces a modification from the linear dependence that is acceptable only for very small values of the related elastic coefficient (see Fig. 4), so its contribution does not seem really relevant;
- The inclusion of the dependence on I_7 or on other coupling terms involving I_5 and I_7 leads to unobserved consequences, mainly for deformations close to the pure uniaxial stretching (i.e., with $\lambda_y = 1$).

Therefore, according to the analysis in [24], the best model appears to be the one that does not include a dependence of the energy on $\mathbb{C}^2$ terms, yielding a nonlinear generalization of Eq. (20).

Also Lazopoulos and Pirentis [19], working in a finite elasticity framework, proposed a model for the cell as a pre-stressed elastic material, whose energy depends only on I_4 but in a non-convex way. Taking into account a misprint, the chosen energy is

$$U = K_1(\mathrm{I}_4 - 1)^2 - K_2(\mathrm{I}_4 - 1)^4 + K_3(\mathrm{I}_4 - 1)^6\,,$$

which gives rise to a co-existence of phases and a saddle-node bifurcation. Thanks to this choice, the model is able to obtain the two symmetric oblique orientations for cells. Instead, in [20] an isotropic Mooney-Rivlin model is used and in [36] a linear elastic model including pre-stresses is deduced focusing on the behaviour of single stress fibres at the microscopic scale. Finally, in [31] the effect of cytoskeletal fluidisation and resolidification is also taken into account. At variance with most experiments, these models yield an equilibrium angle that depends on the applied strain and on the initial orientation. An energetic approach with a wiggly energy to model the attachment of focal adhesions is proposed in [1].

5.3 Temporal Evolution

The models discussed so far mainly focused on the equilibrium orientation of cells, without describing the dynamics of the angle in time. The evolution of cell orientation can be obtained resorting for instance to Lagrangian mechanics arguments, relating the time rate of the orientation angle θ with variations in the virtual work done by the stress acting on the cell due to stress fibre alignment. Considering an overdamped regime, which corresponds to neglecting inertial effects, gives

$$\eta \frac{d\theta}{dt} = -\frac{\partial U}{\partial \theta}(\theta, t)\,, \tag{27}$$

where η is a viscous-like coefficient measuring cell resistance to internal remodelling. Alternatively, Eq. (27) can be thought of as a simple dissipative dynamics, through which the cell evolves to target the minimum of the elastic energy, as done also in [1]. By using the energy in Eq. (19), we can specialize the evolution equation to

$$\begin{aligned}\eta \frac{d\theta}{dt} = \epsilon^2 \Bigg\{ & 4(1-r^2)(K_{\parallel}' - K_{\perp}') \\ & +2(1+r)\left[K_{\parallel}[(r+1)\cos^2\theta - r] + K_{\perp}[(r+1)\cos^2\theta - 1]\right. \\ & \left. -\left(\frac{K_{\phi}}{2} + K_{\parallel\perp}\right)[2(r+1)\cos^2\theta - r - 1]\right\} \sin\theta\cos\theta\,.\end{aligned} \tag{28}$$

Such an equation is for instance used in [1, 22, 42] to get plots like those in Fig. 5, representing the trend of the orientation angle to evolve towards its stable equilibrium θ_{eq} obtained as discussed in Section 5. In the articles treating the cell as a force dipole like those by De and coworkers [11, 12, 34] a similar equation is employed to determine the evolution of the dipole magnitude.

Although the form of Eq. (27) has been postulated on a phenomenological basis in [22], it can also be recovered within a very general remodelling framework, as done in [7]. In this work, the orientation of different types of stress fibres are considered as additional state variables, for which appropriate thermodynamically consistent evolution equations are derived.

Specifically, with reference to Eq. (28), Fig. 5a shows the influence of the stretch amplitude ϵ_0, for a fixed value of the biaxiality ratio. It can be observed that the amplitude modifies the velocity with which reorientation towards the preferential angle happens, and small amplitudes are associated with very slow processes. Instead, the theoretical equilibrium orientation is not altered by variations in ϵ_0 and remains equal to $\pi/4$ due to the fixed value of r. The influence of variations in the biaxiality ratio is reported in Fig. 5b, showing the tendency to evolve towards the stable equilibrium angle predicted by the bifurcation diagram of Fig. 3.

The fact that reorientation happens faster if the stretching amplitude is increased can be readily argued from Eq. (27). In fact, first of all we notice that, in the linear

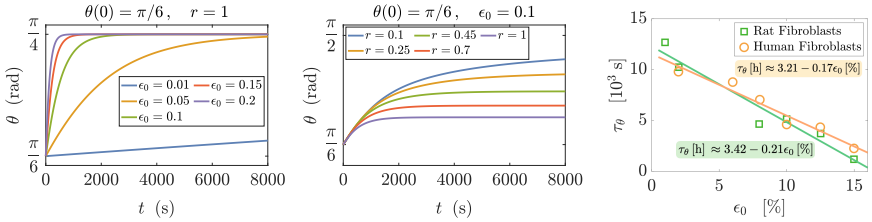

(a) (b) (c)

Fig. 5 Evolution of θ according to Eq. (27) (a) changing ϵ_0 for fixed $r = 1$ and (b) changing r for fixed ϵ_0. (c) Reorientation time as a function of imposed strain. Experimental values are taken from [17].

elastic framework, the elastic strain energy can be written in non-dimensional terms as $U = K_{\parallel}\epsilon^2\bar{U}$, where $\bar{U}$ is dimensionless and independent of ϵ. Hence, one can write the dimensionless evolution equation as

$$\frac{d\theta}{dt} = -\frac{1}{\tau_\theta}\frac{\partial \bar{U}}{\partial \theta}(\theta, t)\,, \tag{29}$$

where $\tau_\theta = \dfrac{\eta}{K_{\parallel}\epsilon^2}$ is a characteristic time that decreases with the stiffness of the material and with the strain magnitude. A similar trend is also obtained in the nonlinear case. Actually, this reasoning predicts that the reorganization time behaves like the inverse of the square of the imposed strain. This might be an explanation of why, for very small amplitudes, reorientation does not happen. Indeed, for $\epsilon \to 0$ the characteristic time would blow up, so that the phenomenon becomes too slow to be observed on the time scale of the experiment and the process is actually hindered by random fluctuations.

However, as shown in Fig. 5c, data in [17] would suggest an almost linear decrease of τ_θ, while the (few) data in [33] seem to suggest that $\tau_\theta \approx \epsilon^{-1.5}$. Though this is not ϵ^{-2}, it still presents a blowing up when $\epsilon \to 0$.

6 Linear Viscoelasticity

As mentioned in the Introduction section, in order to clearly identify a reorientation of cells, the stretching frequency must be sufficiently high. This behaviour cannot be explained by a purely elastic model, which by definition implies an immediate response. Instead, it calls for the introduction of a characteristic response time of the system that needs to be compared with the periodic deformation time scale. The existence of such a characteristic time might be related to the reorganization of the acto-myosin cytoskeleton and of the ensemble of focal adhesions. In this respect, it

is known that the characteristic turnover times of both phenomena are of the order of tens of seconds, or even few minutes (see, for instance, [6]).

At the microscopic level, there are many mathematical models aimed at describing the evolution of stress fibres and focal adhesions, as well as their viscoelastic behaviour. Restricting to models applied to the understanding of cell response under stretch, we mention here the one proposed by Qian et al. [32], who started from the dynamics of nucleation and development of both focal adhesions and stress fibres to describe the formation/disassembly of these sub-cellular structures. Their model monitors changes in the areal density of ligand-receptor bonds in the adhesion cluster and in the density of contracting filaments in the stress fibre. Since disassembly is enhanced by the stress acting on the fibres, they tend to form in the direction which is most favourable energetically.

With the same ideas, Chen et al. [5] proposed a Maxwell-like force-deformation relation, also including the increase of size and strength of focal adhesions with stress to mimic catch-bond behaviours [44].

Working instead in a Continuum Mechanics framework at a macroscopic scale, a viscoelastic model is proposed in [23] to explain why, on the time scale of experiments, the reorientation phenomenon does not occur for small frequencies. The proposed model for the stress $\mathbb{T}(t|\theta)$ at time t, given the history of orientations θ, reads

$$\mathbb{T}(t|\theta) = \int_{-\infty}^{t} \frac{1}{\lambda} e^{-(t-\tau)/\lambda} \mathbb{C}_0(\theta(\tau)) [\mathbb{E}(t) - \mathbb{E}(\tau)] \, d\tau \,, \tag{30}$$

where $\mathbb{C}_0(\theta(\tau))$ is the fourth-order elasticity tensor depending on the orientation angle θ at a past time τ and the exponential is the memory kernel with relaxation time λ (for more details on this type of models the reader can for instance refer to [2] for the isotropic case and to [30] for the anisotropic case). As usual in rheology, for memory kernels of exponential type it is useful to differentiate Eq. (30) and to rewrite the constitutive equation in the following Maxwell-like differential form:

$$\lambda \frac{d\mathbb{T}}{dt}(t|\theta) + \mathbb{T}(t|\theta) = \mathbb{C}_0(t|\theta) \frac{d\mathbb{E}}{dt}(t) \,, \tag{31}$$

where

$$\mathbb{C}_0(t|\theta) := \int_{-\infty}^{t} e^{-(t-\tau)/\lambda} \mathbb{C}_0(\theta(\tau)) \, d\tau = \int_{0}^{+\infty} \lambda e^{-s} \mathbb{C}_0(\theta(t - \lambda s)) \, ds \tag{32}$$

is a functional on the exponentially weighted history of past orientations. We observe that, in the isotropic case, $\mathbb{C}_0$ is twice the so-called elastic viscosity, i.e., the area under the relaxation kernel (times the identity tensor).

Equation (31) is then solved together with an equation for the evolution of θ, governed by the variation of the work done by $\mathbb{T}$ over possible orientations. Assuming again to work in an overdamped regime, one then has

$$\frac{d\theta}{dt}(t) = -\frac{1}{K\lambda_\theta} \frac{\partial \mathbb{T}}{\partial \theta}(t|\theta) : \mathbb{E}(t) \,, \tag{33}$$

where, as in the experiments, the periodic deformation is externally imposed to the specimen, and therefore $\mathbb{E}$ can be taken as independent of θ. In Eq. (33) a characteristic Young modulus K, e.g., $K_\parallel$ encountered in Sec. 5, is introduced to put in evidence the existence of a parameter $\lambda_\theta := \eta/K$ related to the time the cell takes to reorient itself. Moreover, Eq. (33) implies that, for a given strain $\mathbb{E}$, θ tends to assume a value such that the variation of $\mathbb{T}$ with respect to θ either vanishes or becomes orthogonal to $\mathbb{E}$.

In Eqs. (31) and (33) there are two intrinsic characteristic times: λ refers to the viscous behaviour of cells, arising, for instance, from the renewal of focal adhesions with the substratum, while λ_θ is related to the characteristic time of reorganization of stress fibres and consequently to the change in cell orientation. Now, it is useful to discuss how the model behaves when the imposed oscillation period is much shorter or longer than the characteristic remodelling times, which as already mentioned is of the order of tens of seconds/minutes [6]. More in detail, in [23] it is proved that, in the high frequency regime, that corresponds to an imposed cyclic strain faster that the reorganization process, i.e., $\lambda\omega, \lambda_\theta\omega \gg 1$, as characteristic of most successful experiments, one can approximate

$$\mathbb{T}(t|\theta) \approx \mathbb{C}_0(\theta(t))\mathbb{E}_0 e^{i\omega t}. \tag{34}$$

Hence, the stress in such a regime resembles an elastic-like response, as it is classically obtained in viscoelasticity. In this case, therefore, Eq. (33) can be simplified to

$$\frac{d\theta}{dt} = -\frac{1}{\eta}\left[\frac{\partial \mathbb{C}_0}{\partial\theta}\mathbb{E}\right] : \mathbb{E} = -\frac{2}{K\lambda_\theta}\frac{\partial U}{\partial\theta} \tag{35}$$

where

$$U(\theta, t) := \frac{1}{2}\mathbb{E}(t) : \mathbb{C}_0(\theta)\mathbb{E}(t) \tag{36}$$

is the elastic energy. Thus, in the high frequency regime, the change in cell orientation is driven by the minimization of an elastic energy with respect to the orientation angle, as discussed in Section 5.

Conversely, if we consider a low frequency regime in which the period of the cyclic strain imposed to the specimen is much longer than the characteristic time λ of cell relaxation, i.e., $\lambda\omega \ll 1$, the reorientation process is faster than the external oscillations and the cell is able to accommodate the cyclic elongations. In this case, in [23] it is proved that

$$\mathbb{T}(t|\theta) \approx \lambda\overline{\mathbb{C}}_0(t|\theta)\frac{d\mathbb{E}}{dt}(t)\,, \tag{37}$$

corresponding to a viscous-like response, being

$$\overline{\mathbb{C}}_0(t|\theta) := \int_0^{+\infty} s e^{-s}\mathbb{C}_0(\theta(t-\lambda s))\,ds\,.$$

Results of some numerical simulations for this model are shown in Fig. 6, highlighting the role of the frequency in reorientation. As evidenced in Fig. 6a, angular

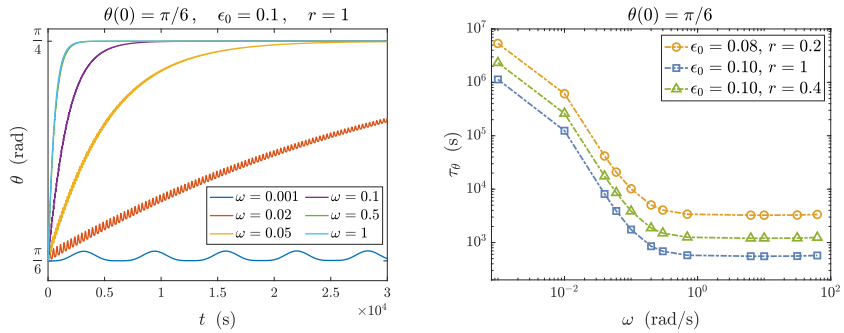

Fig. 6 (a) Evolution of the orientation angle according to Eq. (33) for a fixed biaxiality ratio $r = 1$ and different angular frequencies. When low frequencies are applied, the reorientation process is slow, while for increasing frequencies it rapidly reaches the expected steady state. (b) Plot of the model characteristic time τ_θ as a function of the angular frequency in logarithmic scale, for different values of ϵ_0 and r. Coherently with experiments [17] and with other models [11], a saturation is observed for high frequencies.

frequencies below a minimum threshold, approximately about 0.01 Hz or 0.06 rad/s, lead to very slow reorientation processes and are unable to induce a significantly fast response in cells. Indeed, the reorientation time becomes too slow to be meaningful in comparison with the cell cycle time, and therefore the reorientation process is hindered by random fluctuations. Conversely, for high frequencies the realignment process is initiated, with a characteristic time which is a decreasing function of the frequency, as highlighted by experiments [17]. Such an effect can be observed clearly in Fig. 6b, where the characteristic time τ_θ of the model is plotted as a function of the angular frequency ω in logarithmic scale. However, as the frequency becomes higher, a saturation appears and further increases do not lead to a faster reorientation. This behaviour appears coherent with experimental results [17] and other model outcomes [11].

So, viscoelasticity plays a relevant role when the period of imposed oscillation is much smaller that the relaxation times related to remodelling phenomena in the cell, because it has enough time to adapt. On the other hand, we have shown the robustness of the equilibrium orientation with respect to elastic constitutive relationships.

7 Concluding Remarks

In this Chapter, we have reviewed some mechanics-based approaches that have been proposed in the literature to describe the phenomenon of cell reorientation when the substrate on which they are laid undergoes a periodic stretch.

In Section 5 it was shown that, for a large class of elastic constitutive models, the minimization of the elastic energy best allows to capture the equilibrium orientation

angle as a function of the biaxiality ratio of the imposed deformation and of a dimensionless parameter containing all the mechanical characteristics of the cell and of the substratum.

In order to describe the fact that cell orientation is not observed for too low frequencies of oscillation, in Section 6 a viscoelastic constitutive model was used. This corresponds to taking into account of the remodelling of focal adhesions and of the viscoelastic behaviour of the cytoskeleton. However, this aspect should be further developed in order to include the dynamics of slip bonds and the development of catch bonds in response to the imposed traction. In addition, in all the models reviewed, the active response of the acto-myosin machinery to the imposed deformation is not considered. This might be an important aspect to include, once experiments are available to clarify the related mechanotransduction dynamics.

Acknowledgements This work was partially supported by the Italian National Group of Mathematical Physics (GNFM–INdAM), the Italian Ministry of Education, Universities and Research through the MIUR grant Dipartimenti di Eccellenza 2018–2022, Project No. E11G18000350001, and the Scientific Research Programmes of Relevant National Interest Project No. 2017KL4EF3. GL acknowledges the support of GNFM through the grant *Progetto Giovani 2023* n. CUPE53C22001930001.

Competing Interests The authors have no conflicts of interest to declare that are relevant to the content of this chapter.

References

1. R. Abeyaratne, E. Puntel, and G. Tomassetti. An elementary model of focal adhesion detachment and reattachment during cell reorientation using ideas from the kinetics of wiggly energies. *Journal of Elasticity*, 2022.
2. G. Astarita and G. Marrucci. *Principles of Non-Newtonian Fluid Mechanics*. McGraw-Hill, 1974.
3. V. Barron, C. Brougham, K. Coghlan, E. McLucas, D. O'Mahoney, C. Stenson-Cox, and P.E. McHugh. The effect of physiological cyclic stretch on the cell morphology, cell orientation and protein expression of endothelial cells. *Journal of Materials Science: Materials in Medicine*, 18:1973–1981, 2007.
4. R.C. Buck. Reorientation response of cells to repeated stretch and recoil of the substratum. *Experimental Cell Research*, 127:470–474, 1980.
5. B. Chen, R. Kemkemer, M. Deibler, J. Spatz, and H. Gao. Cyclic stretch induces cell reorientation on substrates by destabilizing catch bonds in focal adhesions. *PLoS ONE*, 7:e48346, 2012.
6. Y. Chen, A.M. Pasapera, A.P. Koretsky, and C.M. Waterman. Orientation-specific responses to sustained uniaxial stretching in focal adhesion growth and turnover. *PNAS*, 110:E2352–E2361, 2013.
7. J. Ciambella, G. Lucci, P. Nardinocchi, and L. Preziosi. Passive and active fiber reorientation in anisotropic materials. *International Journal of Engineering Science*, 176:103688, 2022.
8. P.C. Dartsch, H. Hammerle, and E. Betz. Orientation of cultured arterial smooth muscle cells growing on cyclically stretched substrates. *Acta Anatomica*, 125:108–113, 1986.
9. R. De. A general model of focal adhesion orientation dynamics in response to static and cyclic stretch. *Communications Biology*, 1:81, 2018.

10. R. De and S. Safran. Dynamical theory of active cellular response to external stress. *Physical Review E*, 78:031923–031940, 2008.
11. R. De, A. Zemel, and S. Safran. Do cells sense stress or strain? Measurement of cellular orientation can provide a clue. *Biophysical Journal*, 94:L29–L31, 2008.
12. R. De and S. Zemel, A. Safran. Dynamics of cell orientation. *Nature Physics*, 3:655–659, 2007.
13. U. Faust, N. Hampe, W. Rubner, N. Kirchgessner, S. Safran, B. Hoffmann, and R. Merkel. Cyclic stress at mHz frequencies aligns fibroblasts in direction of zero strain. *PLoS ONE*, 6:e28963, 2011.
14. C. Giverso, N. Loy, G. Lucci, and L. Preziosi. Cell orientation under stretch: A review of experimental findings and mathematical modelling. *Journal of Theoretical Biology*, 572:111564, 2023.
15. L. Gérémie, E. Ilker, M. Bernheim-Dennery, C. Cavaniol, J.-L. Viovy, D.M. Vignjevic, J.-F. Joanny, and S. Descroix. Evolution of a confluent gut epithelium under on-chip cyclic stretching. *Physical Review Research*, 4:023032, 2022.
16. G.A. Holzapfel and R.W. Ogden. Constitutive modelling of passive myocardium: a structurally based framework for material characterization. *Philosophical Transactions of the Royal Society A*, 367:3445–3475, 2009.
17. S. Jungbauer, H. Gao, J.P. Spatz, and R. Kemkemer. Two characteristic regimes in frequency-dependent dynamic reorientation of fibroblasts on cyclically stretched substrates. *Biophysical Journal*, 95:3470–3478, 2008.
18. B.-S. Kim, J. Nikolovski, J. Bonadio, and D.J. Mooney. Cyclic mechanical strain regulates the development of engineered smooth muscle tissue. *Nature Biotechnology*, 17:979–983, 1999.
19. K.A. Lazopoulos and A. Pirentis. Substrate stretching and reorganization of stress fibers as a finite elasticity problem. *International Journal of Solids and Structures*, 44:8285–8296, 2007.
20. K.A. Lazopoulos and D. Stamenovic. A mathematical model of cell reorientation in response to substrate stretching. *MCB*, 3:43–48, 2006.
21. B. Liu, M.-J. Qu, K.-R. Qin, H. Li, Z.-K. Li, B.-R. Shen, and Z.-L. Jiang. Role of cyclic strain frequency in regulating the alignment of vascular smooth muscle cells in vitro. *Biophysical Journal*, 94:1497–1507, 2008.
22. A. Livne, E. Bouchbinder, and B. Geiger. Cell reorientation under cyclic stretching. *Nature Communications*, 5:3938, 2014.
23. G. Lucci, C. Giverso, and L. Preziosi. Cell orientation under stretch: Stability of a linear viscoelastic model. *Mathematical Biosciences*, 337:108630, 2021.
24. G. Lucci and L. Preziosi. A nonlinear elastic description of cell preferential orientations over a stretched substrate. *Biomechanics and Modeling in Mechanobiology*, 20:631–649, 2021.
25. T. Mao, Y. He, Y. Gu, Y. Yang, Y. Yu, X. Wang, and J. Ding. Critical frequency and critical stretching rate for reorientation of cells on a cyclically stretched polymer in a microfluidic chip. *AMS Applied Materials & Interfaces*, 13:13934–13948, 2021.
26. T. Matsumoto, P. Delafontaine, K.J. Schnetzer, B.C. Tong, and R.M. Nerem. Effect of uniaxial cyclic stretch on the morphology of monocytes/macrophages in culture. *Journal of Biomechanical Engineering*, 118:420–422, 1996.
27. M. Morioka, H. Parameswaran, K. Naruse, M. Kondo, M. Sokabe, Y. Hasegawa, B. Suki, and S. Ito. Microtubule dynamics regulate cyclic stretch-induced cell alignment in human airway smooth muscle cells. *PLoS One*, 6:e26384, 2011.
28. R.W. Ogden. Nonlinear elasticity, anisotropy, material stability and residual stresses in soft tissue. In G.A. Holzapfel and R.W. Ogden, editors, *Biomechanics of Soft Tissue in Cardiovascular Systems*, pages 65–108. Springer, 2003.
29. S. Palumbo, A.R. Carotenuto, A. Cutolo, L. Deseri, N. Pugno, and M. Fraldi. Mechanotropism of single cells adhering to elastic substrates subject to exogenous forces. *Journal of the Mechanics and Physics of Solids*, 153:104475, 2021.
30. H.E. Pettermann, C. Cheyrou, and A. DeSimone. Modeling and simulation of anisotropic linear viscoelasticity. *Mechanics of Time-Dependent Materials*, 25:679–689, 2020.

31. A. Pirentis, E. Peruski, A.L. Iordan, and D. Stamenovic. A model for stress fiber realignment caused by cytoskeletal fluidization during cyclic stretching. *Cellular and Molecular Bioengineering*, 4:67–80, 2011.
32. J. Qian, H. Liu, Y. Lin, W. Chen, and H. Gao. A mechanochemical model of cell reorientation on substrates under cyclic stretch. *PLoS ONE*, 8:e65864, 2013.
33. A. Roshanzadeh, T.T. Nguyen, K.D. Nguyen, D.-S. Kim, B.-K. Lee, D.-W. Lee, and E.-S. Kim. Mechanoadaptive organization of stress fiber subtypes in epithelial cells under cyclic stretches and stretch release. *Scientific Reports*, 10:18684, 2020.
34. S. Safran and R. De. Nonlinear dynamics of cell orientation. *Physical Review E*, 80:060901 (R), 2009.
35. A. J. M. Spencer. Constitutive theory for strongly anisotropic solids. In A. J. M. Spencer, editor, *Continuum theory of the mechanics of fibre-reinforced composites*, pages 1–32. Springer, Wien, Austria, 1984.
36. D. Stamenovic, K.A. Lazopoulos, A. Pirentis, and B. Suki. Mechanical stability determines stress fiber and focal adhesion orientation. *Cellular and Molecular Bioengineering*, 2:475–485, 2009.
37. H. Wang, W. Ip, R. Boissy, and E.S. Grood. Cell orientation response to cyclically deformed substrates: experimental validation of a cell model. *Journal of Biomechanics*, 28(12):1543–1552, 1995.
38. J. H.-C. Wang. Substrate deformation determines actin cytoskeleton reorganization: A mathematical modeling and experimental study. *Journal of Theoretical Biology*, 202:33–41, 2000.
39. J. H.-C. Wang, P. Goldschmidt-Clermont, J. Wille, and F. C.-P. Yin. Specificity of endothelial cell reorientation in response to cyclic mechanical stretching. *Journal of Biomechanics*, 34:1563–1572, 2001.
40. J. H.-C. Wang, P. Goldschmidt-Clermont, and F. C.-P. Yin. Contractility affects stress fiber remodeling and reorientation of endothelial cells subjected to cyclic mechanical stretching. *Annals of Biomedical Engineering*, 28:1165–1171, 2000.
41. S. Wang, D. Lu, Z. Zhang, X. Jia, and L. Yang. Effects of mechanical stretching on the morphology of extracellular polymers and the mRNA expression of collagens and small leucine-rich repeat proteoglycans in vaginal fibroblasts from women with pelvic organ prolapse. *PLoS ONE*, 13:e0193456, 2018.
42. G. Xu, X. Feng, and H. Gao. Orientations of cells on compliant substrates under biaxial stretches: A theoretical study. *Biophysical Journal*, 114:701–710, 2018.
43. A. Zemel, I.G. Bischofs, and S. Safran. Active elasticity of gels with contractile cells. *Physical Review Letters*, 97:128103, 2006.
44. C. Zhu. Mechanochemistry: A molecular biomechanics view of mechanosensing. *Annals of Biomedical Engineering*, 42:388–404, 2014.